



LAWRENCE
LIVERMORE
NATIONAL
LABORATORY

LLNL-JRNL-653650

Simulations of Indirectly Driven Gas-Filled Capsules at the National Ignition Facility

S. V. Weber, D. T. Casey, D. C. Eder, J. D. Kilkenny, J. E. Pino, V. A. Smalyuk, G. P. Grim, B. A. Remington, D. P. Rowley, C. B. Yeamans, R. E. Tipton, M. Barrios, R. Benedetti, L. Berzak-Hopkins, D. L. Bleuel, E. J. Bond, D. K. Bradley, J. A. Caggiano, D. A. Callahan, C. J. Cerjan, D. S. Clark, L. Divol, D. H. Edgell, M. J. Edwards, M. J. Eckart, D. Fittinghoff, J. A. Frenje, M. Gatu-Johnson, V. Y. Glebov, S. Glenn, N. Guler, S. W. Haan, A. Hamza, R. Hatarik, H. Herrmann, D. Hoover, W. W. Hsing, N. Izumi, O. S. Jones, M. Kervin, S. Kahn, J. Kline, J. Knauer, A. Kritchler, G. Kyrala, O. L. Landen, S. Le Pape, T. Ma, A. J. Mackinnon, M. M. Marinak, J. M. McNaney, N. B. Meezan, F. E. Merrill, M. Mintz, A. Moore, D. H. Munro, A. Nikroo, A. Pak, T. Parham, et al.

April 28, 2014

Physics of Plasmas

Disclaimer

This document was prepared as an account of work sponsored by an agency of the United States government. Neither the United States government nor Lawrence Livermore National Security, LLC, nor any of their employees makes any warranty, expressed or implied, or assumes any legal liability or responsibility for the accuracy, completeness, or usefulness of any information, apparatus, product, or process disclosed, or represents that its use would not infringe privately owned rights. Reference herein to any specific commercial product, process, or service by trade name, trademark, manufacturer, or otherwise does not necessarily constitute or imply its endorsement, recommendation, or favoring by the United States government or Lawrence Livermore National Security, LLC. The views and opinions of authors expressed herein do not necessarily state or reflect those of the United States government or Lawrence Livermore National Security, LLC, and shall not be used for advertising or product endorsement purposes.

Simulations of indirectly driven gas-filled capsules at the National Ignition Facility

S. V. Weber,¹ D. T. Casey,¹ D. C. Eder,¹ J. D. Kilkenny,⁵ J. E. Pino,¹ V. A. Smalyuk,¹ G. P. Grim,² B. A. Remington,¹ D. P. Rowley,¹ C. B. Yeamans,¹ R. E. Tipton,¹ M. Barrios,¹ R. Benedetti,¹ L. Berzak Hopkins,¹ D. L. Bleuel,¹ E. J. Bond,¹ D. K. Bradley,¹ J. A. Caggiano,¹ D. A. Callahan,¹ C. J. Cerjan,¹ D. S. Clark,¹ L. Divol,¹ D. H. Edgell,³ M. J. Edwards,¹ M. J. Eckart,¹ D. Fittinghoff,¹ J. A. Frenje,⁴ M. Gatu-Johnson,⁴ V. Y. Glebov,³ S. Glenn,¹ N. Guler,² S. W. Haan,¹ A. Hamza,¹ R. Hatarik,¹ H. Herrmann,² D. Hoover,⁵ W. W. Hsing,¹ N. Izumi,¹ O. S. Jones¹, M. Kervin,¹ S. Khan,¹ J. Kline,² J. Knauer,³ A. Kritchler,¹ G. Kyrala,² O. L. Landen,¹ S. Le Pape,¹ T. Ma,¹ A. J. Mackinnon,¹ M. M. Marinak,¹ J. M. McNaney,¹ N. B. Meezan¹, F. E. Merrill,² M. Mintz,¹ A. Moore,⁶ D. H. Munro,¹ A. Nikroo,⁵ A. Pak,¹ T. Parham,¹ R. Petrasso,⁴ H. G. Rinderknecht,⁴ D. B. Sayre,¹ S. M. Sepke,¹ B. K. Spears,¹ W. Stoeffl,¹ R. Tommasini,¹ R. P. Town,¹ P. Veligov,² K. Widmann,¹ D. C. Wilson,² and A. B. Zylstra⁴

1) Lawrence Livermore National Laboratory, Livermore, CA 94550

2) Los Alamos National Laboratory, Los Alamos, NM 87545

3) Laboratory for Laser Energetics, University of Rochester, Rochester, NY 14623

4) Massachusetts Institute of Technology, Cambridge, MA 02139

5) General Atomics, San Diego, CA 92121

6) AWE Aldermaston, Reading, Berkshire, RG7 4PR, United Kingdom.

ABSTRACT

Gas-filled capsules imploded with indirect drive on the National Ignition Facility have been employed as symmetry surrogates for cryogenic-layered ignition capsules and to explore interfacial mix. Plastic capsules containing CD layers and filled with tritium gas provide a direct measure of mix of ablator into the gas fuel. Other plastic capsules have employed DT or D³He gas fill. We present the results of two-dimensional simulations of gas-filled capsule implosions with known degradation sources of time-dependent drive asymmetry, the capsule support tent, roughness at material interfaces, and prescribed gas-ablator interface mix. Unlike the case of cryogenic-layered implosions, many observables of gas-filled implosions are matched by these simulations. Yields of TT and DT neutrons as well as other x-ray and nuclear diagnostics are matched for CD-layered implosions. Yields of DT-filled capsules are over-predicted by factors of 1.4-2, while D³He capsule yields are matched, as well as other metrics for both capsule types.

I. INTRODUCTION

The goal of inertial confinement fusion (ICF)^{1,2} is to implode a capsule containing DT fuel so that the hot spot achieves sufficient temperature and density to ignite thermonuclear reactions and propagate into colder, denser fuel to achieve high gain. The current indirect-drive ignition design at the National Ignition Facility³⁻⁵ employs a CH ablator over a layer of DT ice surrounding gas in vapor pressure equilibrium. Implosions of capsules based upon the circa-2012 ignition design gave yields well below expectations^{6,7}, even from simulations including known sources of degradation^{8-9,11}.

Layered implosions began in 2013, using a different “high foot” laser pulse, which results in a higher adiabat¹², performed nearer to simulations. We will not discuss experiments with the high foot pulse in this report.

Capsules filled with DT gas but without a condensed DT layer do not offer the potential of high gain, but have been imploded on NIF for various purposes. Gas-filled CH capsules, with the ablator thickened to compensate for the mass of the missing DT ice layer, have been employed as symmetry surrogates of ignition capsules, “SymCaps”¹³. NIF SymCaps were most often filled with 30% D, 70% ³He so as to still provide nuclear diagnostic information through the D-³He mirror reaction of DT fusion, but to also increase x-ray emission compared to hydrogen fuel. Several have been fielded with DT fuel in varying isotopic proportion, allowing for wider range nuclear observables while still allowing for substantial x-ray diagnostic signal¹⁴. Recently, plastic capsules with CD layers and tritium gas fuel have been used to measure atomic mix between ablator and fuel¹⁵⁻²².

SymCaps are most often driven with the same multi-step laser pulses designed for cryo-layered ignition capsules so as to replicate the hohlraum dynamics and consequent time-dependent symmetry of the x-ray drive. The steps are tuned so that several shocks merge just below the inner surface of the ice layer²⁴. When a gas-filled capsule is driven with the same pulse, the shocks transit the mass-equivalent CH layer in less time than the four times thicker DT ice layer and the inner surface releases before the next shock arrives, giving less than optimal compression of the ablator.

The experimental series employing CD layers and tritium gas fill is described in more detail elsewhere^{21,22}. Variations of this technique were used previously on NOVA

and OMEGA¹⁵⁻²⁰. Atomic mix between the ablator and gas is needed to give DT reactions, which are diagnosed by the 14 MeV neutrons. A 4 μm thick CD layer was placed either adjacent to the gas or recessed by 1, 2, 4, or 8 μm . Earlier publications compare experimental results with the K-L dynamic mix²⁵ model in the code ARES²⁶. The work-horse simulation code employed for ICF research at LLNL is HYDRA²⁷. Design calculations for NIF ignition have primarily employed HYDRA while ARES has very rarely been employed for this purpose. Therefore, it is of interest to investigate the simulation methodology used for ignition design performs when applied to this experimental platform. HYDRA does not supply a dynamic mix model (by which we mean one based upon differential equations) but allows the user to specify a time-dependent mix depth.

We have simulated the CD layer implosions using HYDRA and including known sources of degradation, time-dependent radiation drive asymmetry, a mock-up of the effect of the capsule support tent, roughness of ablator interfaces, and a mix prescription. We are able to match capsule performance by adjusting a single parameter controlling the mix depth. The same model predicts larger-than-measured yields, but matches many metrics of the performance of DT and D³He-filled gas capsules as well as the reproducibility of the data. We shall present application of our model to CD layer capsules in Section II. Extension to DT and D³He-filled gas capsules is found in Section III. Section IV gives conclusions.

II. SIMULATIONS OF IMPLOSIONS WITH CD LAYERS

The CD layer implosion series used CH capsules with a nominal diameter of 2280 μm and 209- μm thickness. Si-doped layers were used to mitigate the effect of Au M-

band preheat. A CD layer of 4 μm thickness was placed next to the gas or offset by 1.2, 2.3, 3.9, or 8.0 μm . The shells were filled with tritium gas of density 11.05 mg/cm³ with a small contamination of deuterium of about 0.1% by atom fraction. The DT yield from D contamination is a background to the signal from mix, and was measured in two shots without CD layers. Another control experiment used D_{0.75}T_{0.25} gas fill at density 8.29 mg/cm³. All implosions employed nominally the same laser pulse, a 4-step pulse with 1.5 MJ, peak power 435 TW, which also had been used in a number of cryo-layered DT implosions.

The performance of the implosions was measured with a multitude of nuclear and x-ray diagnostics²⁸. Hohlraum drive as measured by the Dante diagnostic²⁹ was very repeatable, Tr = 294±4 eV. Capsule x-ray bang times^{30,31} were ~22.55±0.10 ns, all within 100 ps. We will focus upon capsule performance metrics of DT, DD, TT neutron yield³²⁻³⁴, neutron time-of-flight measurements³⁵ of ion temperature³⁶ and down-scatter ratio (DSR), temporal burn width from x-rays³⁷ or DT gammas^{38,39}, and x-ray⁴⁰ and neutron image size and shape⁴¹. DSR is the ratio of neutrons in the 10-12 MeV energy range to those in the 13-15 MeV range, and is diagnostic of fuel column density⁴².

Simulations with the HYDRA code were two-dimensional with axial symmetry, of the capsule only, and were driven with frequency-dependent sources linked from post-shot integrated simulations⁹. The sources included time-dependent drive asymmetry in Legendre modes up to 8 based upon capsule ablation pressure taken from the integrated simulations. The integrated simulations used measured beam quad powers for each shot. Measured backscatter was removed from the incident laser power, and predicted effects of cross-beam radiation transfer were included. Incident power levels also were modified

with time-dependent multipliers so as to match VISAR shock and capsule limb position measurements on shots employing the same laser pulse. The effect of the 110 nm-thick capsule support web was mocked up by imposing grooves on the outside of the ablator of cosine shape, 350 μm wavelength, and 0.2 μm depth at the 45° latitude where the tent separates from the capsule. These parameters were tuned to match the appearance of the groove feature in backlit shell images at \sim 250 μm shell radius¹⁰. Roughness at the NIF revision 5 specification³ was included on all ablator interfaces, including interfaces between dopant levels. Roughness seeded at the ablator outer surface dominated over perturbations seeded at other interfaces.

Because HYDRA reconstructs material interfaces, none of these perturbations would create any atomic mix between the ablator and fill gas without the addition of an interface mix model. Mix around the ablator-gas interface was imposed out to specified fractions of the separation of the “fall-line” from the interface. The fall line is a linear extrapolation of the interface motion at peak velocity. This scaling is motivated by the Rayleigh-Taylor (RT) result of Read⁴³ and Youngs^{44,45}

$$h_b = \alpha A g t^2$$

where h_b is the bubble height, A the Atwood number, g acceleration, t time, and α is a constant. From this it follows that the mix penetration on the bubble side is a fraction $f_b = 2\alpha A$ of the fall line separation, which is $1/2gt^2$. The ratio of penetration on the gas or “spike” side of the interface to that on the ablator or “bubble” side was specified⁴⁶ as $f_s/f_b = 1+A = 1.3$, using 0.3 as the Atwood number.

The fuel-ablator interface is subjected to series of shocks and intervals of variable acceleration of both signs so the classical RT result is not directly applicable; the fall line

fraction mix prescription was employed as a convenient and physically-motivated parameterization. Haan⁴⁶ shows such scaling is observed for his multi-wavelength saturation model as applied to specific cases.

The imposed isotope fractions were linear across the specified mix region limits. The HYDRA simulation mixes materials only in the radial mesh coordinate direction. In order to couple the interface mix model with the effect of resolved perturbations, the mix boundaries were averaged over the transverse mesh direction for 100 iterations. The simulations employed 1024 zones in π radians so the transverse averaging was effectively a low pass filter with a cut-off mode number of ~ 20 .

Figure 1 shows material density on the right and the product of deuteron and triton number densities on the left for a typical simulation of a CD shell implosion with no offset of the CD layer. The effects of all four perturbation sources - drive asymmetry, the support tent, surface roughness, and the interface mix model - are all clearly apparent. Atomic mix of D and T occurs in a thin annulus of ~ 20 μm thickness which follows the distortion of the fuel region resulting from the other three seeds.

Figure 2 shows the TT and DT yields as functions of the CD layer offset for different values of f_b . The TT yield comes from the entire gas volume and does not depend upon the location of the CD layer. The DT yield comes only from the region of gas-ablator mix, and drops with increasing layer recession until at 8 μm recession it approaches the background due to deuterium contamination in the T_2 gas. A fall-line fraction of $f_b = 0.04$ gives a fair fit to both TT and DT experimental yields. For $A=0.3$, this corresponds to Read and Youngs $\alpha = 0.06$. Figure 2c shows the ion temperature inferred from DT neutrons. It is not possible to infer a temperature from TT neutrons

because of the broad 3-body spectrum. The background experiment gave a temperature of ~ 3 keV which is a burn-weighted temperature for the entire gas volume. The DT burn temperature with the CD layer probes the mix region, which was cooler, ~ 2 keV. As the layer is offset is increased, the ion temperature rises back to that of the background shots suggesting that DT yield is increasingly dominated by the contamination contribution. It cannot be inferred that mix lowered the temperature of the same mass element of gas as the DT yield came from the outer edge of the gas for the CD layer experiments compared to the entire volume for the control shots. X-ray metrics for these shots were similar to those of the corresponding DT shot N120923, which is discussed below.

The ARES model parameter fit for these shots^{21,22} used an enhanced surface roughness of three times nominal to match the experimental data. Fig. 4 shows the fall-off of simulated yield for our model as the surface roughness is increased. We judge nominal roughness to be a satisfactory fit. However, the threefold nominal result matches the DT measurement better than nominal does but agrees more poorly with the TT measurement, so the overall agreement is similar to nominal roughness.

III. EXTENSION TO DT- AND D³HE-FILLED CAPSULES

The same simulation model was applied to four DT gas-filled implosions employing the fall line mix fraction as fit to the CD layer experiments. One, NIF shot N120923, had 75% D and 25% T but was otherwise equivalent to the CD layer shots, including its laser pulse shape. Shot N130505 used the same 439 TW peak power but with the pulse shortened to lower the energy to 1.3 MJ. Shot N130507 used lower peak power of 360 TW, but a longer pulse to give the same 1.3 MJ energy as N130505. Also, it employed a hohlraum which was 700 μm longer than those of the other shots discussed

here. Shot N130503²² used a single-shock pulse of 918 kJ in 4.3 ns with 16 torr He near-vacuum hohlraum gas fill. This implosion had lower convergence, CR ~ 6 and was nearly an exploding pusher.

Table 1 shows simulated and measured values of thirteen nuclear and x-ray diagnostic metrics for these four shots. This model reproduces the DT and DD neutron yields, ion temperatures, gamma and x-ray burn widths, gamma and x-ray image sizes, and image elongation P2/P0. The simulated yields are 1.4-2 times larger than the measured values for the ablatively-driven capsules. Agreement in image shape is a test of the integrated hohlraum simulations providing the drive asymmetry rather than of the capsule model which is the subject of this work, but correct shape was desired to include the influence upon other metrics. Ion temperatures, burn widths, down-scatter ratios, and image sizes generally agree with data nearly as well as the data is reproduced between equivalent shots. We disagree substantially on the down-scatter ratio for the exploding pusher although we fit the x-ray and neutron image sizes. Generally, our x-ray image sizes are a little larger than measured although our neutron image sizes match measurements better. Figure 3 compares simulated and measured x-ray and neutron images for shot N120923. The simulation gets the x-ray size and elongation approximately correctly but does not predict the internal structure. Time-dependent imaging shows bright spots moving from the edge to the center, which are believed to be 3-D jets, which these simulations cannot reproduce. The simulated structure is more nearly correct for the neutron image. The 17% contour for the simulated image follows extensions toward top and bottom while similar extensions in the experimental neutron image have lower intensity and are not picked up by the 17% contour.

Figure 5 shows the progressive effect of the four degradation seeds for shot N130507. The 1-D clean yield is about 2.5 times that of the full 2-D model. Surface roughness is the largest single degradation, reducing the yield by nearly 40%. Drive asymmetry is only about a 3% effect for this case. The tent causes a 23% yield reduction in this model. The fall line mix model with $f_b=0.04$ by itself reduces the simulated yield by only 13%. A different drive model from Clark⁸, which was adjusted to match inflight shell measurements, gives a yield 11% lower than the drive taken directly from integrated hohlraum simulations. The measured DT yield for this shot was 54% of the yield of the nominal 2-D model, or 61% of the yield with the Clark drive.

Figure 6 shows how the simulated DT yield of shot N130507 drops as the surface roughness is increased. The measured yield is matched at a roughness multiplier of about 5. The DD yield and ion temperature are also matched for the same multiplier. Other performance metrics listed in Table I are about the same as for nominal roughness.

Most often NIF SymCaps were fielded with D³He fill, usually in 30:70 proportion, to avoid tritium handling. There were five shots with equivalent capsules and pulses as the CD mix series. Three of these (N120906, N120909, N120910) gave DD yields of $6.06\text{--}6.99 \times 10^{11}$, while two had lower yields, N111120 - 5.1×10^{11} , N120729 - 3.5×10^{11} . The laser pulses of all five shots agreed to within 5% in the foot, 2% in the peak. Capsule dimensions were well matched, within 14 μm in inner radius 1.5 μm in thickness. Capsule surface finishes ranged from 0.8 – 1.4 times the NIF specifications for Legendre modal bands spanning 2-25, and 0.5-0.6 times the specification for the modal band 26-150. We were unable to identify any feature of the lower-performing shots which set them apart. It is possible that the similar yields of the three shots taken within a

week were fortuitous and that NIF SymCap yields are reproducible only to within a factor 2, between extremes, for identical shots.

The shots are sufficiently similar that a single simulation applies to all five. The simulated yield of 5.5×10^{11} falls in the middle of the measured values, within 15% of three of the shots and within 40% of all. Table II compares performance metrics of shot N120909 with the model. Performance metrics besides DD yield are similar for the other four shots. Agreement of the model with performance metrics for the D³He SymCaps is quite good.

Figure 7 shows simulated and measured x-ray images for D³He fill shot N120909. The simulation captures the more centrally peaked emission for D³He fill as compared with hydrogen, as well as approximating the size and elongation of the 17% contour.

IV. CONCLUSIONS

A two-dimensional simulation model including expected degradation sources of interface roughness, time-dependent radiation drive asymmetry, a mock up of the support tent, and an interface mix prescription is able to match the performance of tritium-filled capsules with a CD layer recessed different distances from the interface with the fill gas. The same model matches the performance of capsules filled with D³He gas. The model also matches many performance metrics of capsules with DT gas fill. However, the model over-predicts the DT yield of those capsules by up to a factor of two.

The yields of the ablatively-driven DT capsules can be matched by increasing the surface roughness in the models by a factor of about 5. This factor does not seem to be necessary for TT or D³He-filled capsules. This could be evidence of isotope separation⁴⁷, or perhaps these three specific shots performed more poorly, like the D³He shot

N120729. Clark et al.⁸ found that a factor of 5 enhancement in roughness matched the yield of a specific DT-layered capsule, which was more than a factor of 10 below the prediction for nominal roughness. Layered capsules are much more sensitive to degradation sources, likely because of higher convergence and otherwise differing dynamics from gas-filled implosions.

The capsules employed for these shots could not have been this rough, but the growth factors of perturbations could be higher than simulated or there could be additional growth seeds not represented in the model. The calculated growth factor of ablation front perturbations to the time of peak velocity is ~ 1000 for these SymCaps⁴⁸, so an additional factor of 5 is only 20% more e-foldings of growth. Three-dimensional growth is expected to be larger than 2-D only by perhaps 50% in total penetration in the nonlinear regime⁴⁹, not enough to account for the discrepancy.

One might ask whether the mix prescription employed in this study would affect simulated performance of layered implosions. Unfortunately, the interface mix prescription used here for gas-filled capsules has little effect upon the yield of layered implosions which do not ignite, such as all those to date for NIF. The hot spot in layered implosions is separated from the ablator by cold DT, so mix of modest extent about the inner surface of the ablator does not penetrate into the hot spot. The yield of an igniting capsule would be degraded by pollution of the cold fuel. There is no material interface between the cold DT and the hot spot about which an analogous mix prescription could be used.

Ongoing experiments are measuring growth of applied surface perturbations to test the growth predicted by simulations⁵⁰. Efforts to improve drive symmetry and reduce

the effect of the tent are also under way. However, a pronounced improvement in yield may not be apparent in gas-filled capsules because their performance may not be sufficiently sensitive. Only cryo-layered implosions may confirm definitively the improvement in implosion uniformity.

ACKNOWLEDGMENTS

This work would not be possible without the efforts of a very large team of NIF diagnostic scientists, operations staff, target fabricators, and program management.

This work was performed under the auspices of the U.S. Department of Energy by Lawrence Livermore National Laboratory under Contract DE-AC52-07NA27344.

REFERENCES

- ¹S. Atzeni and J. Meyer-ter-Vehn, *The Physics of Inertial Fusion: Beam Plasma Interaction, Hydrodynamics, Hot Dense Matter*, International Series of Monographs on Physics (Clarendon Press, Oxford, 2004).
- ²J. D. Lindl, *Inertial Confinement Fusion: The Quest for Ignition and Energy Gain Using Indirect Drive* (Springer-Verlag, New York, 1998).
- ³S. W. Haan, J. D. Lindl, D. A. Callahan, D. S. Clark, J. D. Salmonson, B. A. Hammel, L. J. Atherton, R. C. Cook, M. J. Edwards, S. Glenzer, A. V. Hamza, S. P. Hatchett, M. C. Herrmann, D. E. Hinkel, D. D. Ho, H. Huang, O. S. Jones, J. Kline, G. Kyrala, O. L. Landen, B. J. MacGowan, M. M. Marinak, D. D. Meyerhofer, J. L. Milovich, K. A. Moreno, E. I. Moses, D. H. Munro, A. Nikroo, R. E. Olson, K. Peterson, S. M. Pollaine, J. E. Ralph, H. F. Robey, B. K. Spears, P. T. Springer, L. J. Suter, C. A. Thomas, R. P. Town, R. Vesey, S. V. Weber, H. L. Wilkens, and D. C. Wilson Phys. Plasmas **18**, 051001 (2011).

⁴E. I. Moses, R. N. Boyd, B. A. Remington, C. J. Keane, and R. Al-Ayat, *Phys. Plasmas* **16**, 041006 (2009);

⁵G. H. Miller, E. I. Moses and C. R. Wuest, *Opt. Eng.* **44**3, 2841 (2004).

⁶S. P. Regan, R. Epstein, B. A. Hammel, L. J. Suter, J. Ralph, H. Scott, M. A. Barrios, D. K. Bradley, D. A. Callahan, C. Cerjan, G. W. Collins, S. N. Dixit, T. Doeppner, M. J. Edwards, D. R. Farley, S. Glenn, S. H. Glenzer, I. E. Golovkin, S. W. Haan, A. Hamza, D. G. Hicks, N. Izumi, J. D. Kilkenny, J. L. Kline, G. A. Kyrala, O. L. Landen, T. Ma, J. J. MacFarlane, R. C. Mancini, R. L. McCrory, N. B. Meezan, D. D. Meyerhofer, A. Nikroo, K. J. Peterson, T. C. Sangster, P. Springer and R. P. J. Town, *Phys. Plasmas* **19**, 056307 (2012).

⁷T. Ma, P.K. Patel, N. Izumi, P.T. Springer, M.H. Key, L.J. Atherton, L.R. Benedetti, D.K. Bradley, D.A. Callahan, P.M. Celliers, C.J. Cerjan, D.S. Clark, E.L. Dewald, S.N. Dixit, T. Doppner, D.H. Edgell, R. Epstein, S. Glenn, G. Grim, S.W. Haan, B.A. Hammel, D. Hicks, W.W. Hsing, O.S. Jones, S.F. Khan, J.D. Kilkenny, J.L. Kline, G.A. Kyrala, O.L. Landen, S. Le Pape, B.J. MacGowan, A.J. Mackinnon, A.G. MacPhee, N.B. Meezan, J.D. Moody, A. Pak, T. Parham, H.-S. Park, J.E. Ralph, S.P. Regan, B.A. Remington, H.F. Robey, J.S. Ross, B.K. Spears, V. Smalyuk, L.J. Suter, R. Tommasini, R.P. Town, S.V. Weber, J.D. Lindl, M.J. Edwards, S.H. Glenzer, and E.I. Moses, *Phys. Rev. Lett.* **111**, 085004 (2013).

⁸D. S. Clark, D. E. Hinkel, D. C. Eder, O. S. Jones, S. W. Haan, B. A. Hammel, M. M. Marinak, J. L. Milovich, H. F. Robey, L. J. Suter and R. P. J. Town, *Phys. Plasmas* **20**, 056318 (2013).

⁹O. S. Jones, C. J. Cerjan, M. M. Marinak, J. L. Milovich, H. F. Robey, P. T. Springer, L. R. Benedetti, D. L. Bleuel, E. J. Bond, D. K. Bradley, D. A. Callahan, J. A. Caggiano, P. M. Celliers, D. S. Clark, S. M. Dixit, T. Doppner, R. J. Dylla-Spears, E. G. Dzentitis, D. R. Farley, S. M. Glenn, S. H. Glenzer, S. W. Haan, B. J. Haid, C. A. Haynam, D. G. Hicks, B. J. Kozioziemski, K. N. LaFortune, O. L. Landen, E. R. Mapoles, A. J. MacKinnon, J. M. McNaney, N. B. Meezan, P. A. Michel, J. D. Moody, M. J. Moran, D. H. Munro, M. V. Patel, T. G. Parham, J. D. Sater, S. M. Sepke, B. K. Spears, R. P. J. Town, S. V. Weber, K. Widmann, C. C. Widmayer, E. A. Williams, L. J. Atherton, M. J. Edwards, J. D. Lindl, B. J. MacGowan, L. J. Suter, R. E. Olson, H. W. Herrmann, J. L. Kline, G. A. Kyrala, D. C. Wilson, J. Frenje, T. R. Boehly, V. Glebov, J. P. Knauer, A. Nikroo, H. Wilkens and J. D. Kilkenny, Phys. Plasmas **19**, 056315 (2012).

¹⁰S. W. Haan, L. Berzak Hopkins, D. S. Clark, D. Eder, B. A. Hammel, A. Hamza, D. Ho, O. S. Jones, A. Kritch, K. LaFortune, B. J. MacGowan, N. B. Meezan, J. Milovich, J. L. Peterson, H. F. Robey, J. D. Salmonson, B. K. Spears, R. P. Town, J. L. Kline, D. C. Wilson, A. N. Simakov, S. A. Yi, A. Nikroo, H. Huang and H. Hoover, Bull. Am. Phys. Soc. **58**, 155 (2013).

¹¹B. K. Spears, S. Glenzer, M. J. Edwards, S. Brandon, D. Clark, R. Town, C. Cerjan, R. Dylla-Spears, E. Mapoles, D. Munro, J. Salmonson, S. Sepke, S. Weber, S. Hatchett, S. Haan, P. Springer, E. Moses, J. Kline, G. Kyrala and D. Wilson, Phys. Plasmas **19**, 056316 (2012).

¹²O. A. Hurricane, D. A. Callahan, D. T. Casey, P. M. Celliers, C. Cerjan, E. L. Dewald, T. R. Dittrich, T. Döppner, D. E. Hinkel, L. F. Berzak Hopkins, J. L. Kline, S.

Le Pape, T. Ma, A. G. MacPhee, J. L. Milovich, A. Pak, H.-S. Park, P. K. Patel, B. A. Remington, J. D. Salmonson, P. T. Springer and R. Tommasini, *Nature* 13008 (2014).

¹³G. A. Kyrala, J. L. Kline, S. Dixit, S. Glenzer, D. Kalantar, D. Bradley, N. Izumi, N. Meezan, O. Landen, D. Callahan, S. V. Weber, J. P. Holder, S. Glenn, M. J. Edwards, J. Koch, L. J. Suter, S. W. Haan, R. P. J. Town, P. Michel, O. Jones, S. Langer, J. D. Moody, E. L. Dewald, T. Ma, J. Ralph, A. Hamza, E. Dzenitis, and J. Kilkenny, *Phys. Plasmas* **18**, 056307.

¹⁴J. D. Kilkenny, J. A. Caggiano, R. Hatarik, J. P. Knauer, D. B. Sayre, B. K. Spears, S. V. Weber, C. B. Yeamans, C. J. Cerjan, L. Divol, M. J. Eckart, V. Yu. Glebov, H. W..Herrmann, S. Le Pape, D. H. Munro, G. P. Grim, O. S. Jones, L. Berzak-Hopkins, M. Gatu-Johnson, A. J. Mackinnon, N. B. Meezan, D. T. Casey, J. A. Frenje, J. M. McNaney, R. Petrasso, H. Rinderknecht, W. Stoeffl and A. B. Zylstra, “Understanding the stagnation and burn of implosions on NIF”, 2013 IFSA proceedings, in press (2014).

¹⁵D. C. Wilson, P. S. Ebey, T. C. Sangster, W. T. Shmayda, V. Yu. Glebov and R. A. Lerche, *Phys. Plasmas* **18**, 112707 (2011).

¹⁶D. D. Meyerhofer, J. A. Delettrez, R. Epstein, V. Yu. Glebov, V. N. Goncharov, R. L. Keck, R. L. McCrory, P. W. McKenty, F. J. Marshall, P. B. Radha, S. P. Regan, S. Roberts, W. Seka, S. Skupsky, V. A. Smalyuk, C. Sorce, C. Stoeckl, J. M. Soures, R. P. J. Town, B. Yaakobi, J. D. Zuegel, J. Frenje, C. K. Li, R. D. Petrasso, F. H. Séguin, K. Fletcher, S. Padalino, C. Freeman, N. Izumi, R. Lerche, T. W. Phillips and T. C. Sangster, *Phys. Plasmas* **8**, 2251 (2001).

¹⁷P. B. Radha, J. Delettrez, R. Epstein, V. Yu Glebov, R. Keck, R. L. McCrory, P. McKenty, D. D. Meyerhofer, F. Marshall, S. P. Regan, S. Roberts, T. C. Sangster, W.

Seka, S. Skupsky, V. Smalyuk, C. Sorce, C. Stoeckl, J. Soures, R. P. J. Town, B. Yaakobi, J. Frenje, C. K. Li, R. Petrasso, F. Seguin, K. Fletcher, S. Padalino, C. Freeman, N. Izumi, R. Lerche and T. W. Phillips, Phys. Plasmas **9**, 2208 (2002).

¹⁸C. K. Li, F. H. Séguin, J. A. Frenje, S. Kurebayashi, R. D. Petrasso, D. D. Meyerhofer†, J. M. Soures, J. A. Delettrez, V. Yu. Glebov, P. B. Radha, S. P. Regan, S. Roberts, T. C. Sangster, and C. Stoeckl, Phys. Rev. Lett. **89**, 165002 (2002).

¹⁹J. R. Rygg, J. A. Frenje, C. K. Li, F. H. Séguin, R. D. Petrasso, V. Yu. Glebov, D. D. Meyerhofer†, T. C. Sangster, and C. Stoeckl, Phys. Rev. Lett. **98**, 215002 (2007).

²⁰R. E. Chrien N. M. Hoffman, J. D. Colvin, C. J. Keane, O. L. Landen and B. A. Hammel, Phys. Plasmas **5**, 768 (1998).

²¹V. A. Smalyuk, R. E. Tipton, J. E. Pino, D. T. Casey, G. P. Grim, B. A. Remington, D. P. Rowley, S. V. Weber, M. Barrios, R. Benedetti, D. L. Bleuel, D. K. Bradley, J. A. Caggiano, D. A. Callahan, C. J. Cerjan, D. S. Clark, D. H. Edgell, M. J. Edwards, J. A. Frenje, M. Gatuz-Johnson, V. Y. Glebov, S. Glenn, S. W. Haan, A. Hamza, R. Hatarik, W. W. Hsing, N. Izumi, S. Khan, J. D. Kilkenny, J. Kline, J. Knauer, O. L. Landen, T. Ma, J. M. McNaney, M. Mintz, A. Moore, A. Nikroo, A. Pak, T. Parham, R. Petrasso, D. B. Sayre, M. B. Schneider, R. Tommasini, R. P. Town, K. Widmann, D. C. Wilson, and C. B. Yeamans *Phys. Rev. Lett.* In press (2014).

²²D. T. Casey, V. A. Smalyuk, R. E. Tipton, J. E. Pino, G. P. Grim, B. A. Remington, D. P. Rowley, S. V. Weber, M. Barrios, R. Benedetti, D. L. Bleuel, E. J. Bond, D. K. Bradley, J. A. Caggiano, D. A. Callahan, C. J. Cerjan, D. H. Edgell, M. J. Edwards, D. Fittinghoff, J. A. Frenje, M. Gatuz-Johnson, V. Y. Glebov, S. Glenn, N. Guler, S. W. Haan, A. Hamza, R. Hatarik, H. Herrmann, D. Hoover, W. W. Hsing, N. Izumi, P.

Kervin, S. Khan, J. D. Kilkenny, J. Kline, J. Knauer, G. Kyrala, O. L. Landen, T. Ma, J. M. McNaney, M. Mintz, A. Moore, A. Nikroo, A. Pak, T. Parham, R. Petrasso, H. G. Rinderknecht, D. B. Sayre, M. Schneider, R. Tommasini, R. P. Town, K. Widmann, D. C. Wilson, and C. B. Yeamans, submitted to *Phys. Plasmas*.

²³L. Berzak Hopkins et al. submitted to *Phys. Plasmas*.

²⁴D. H. Munro, P. M. Celliers, G. W. Collins, D. M. Gold, L. B. Da Silva, S. W. Haan, R. C. Cauble, B. A. Hammel, and W. W. Hsing, *Phys. Plasmas* **8**, 2245 (2001).

²⁵G. Dimonte and R. Tipton, *Phys. Fluids* **18**, 085101 (2006).

²⁶R. M. Darlington, T. L. McAbee, and G. Rodriguez, *Comput. Phys. Commun.* **135**, 58 (2001).

²⁷M. M. Marinak, R. E. Tipton, O. L. Landen, T. J. Murphy, P. Amendt, S. W. Haan, S. P. Hatchett, C. J. Keane, R. McEachern, and R. Wallace, *Phys. Plasmas* **3**, 2070 (1996).

²⁸M. G. Johnson, J. A. Frenje, D. T. Casey, C. K. Li, F. H. Séguin, R. Petrasso, R. Ashabrunner, R. M. Bionta, D. L. Bleuel, E. J. Bond, J. A. Caggiano, A. Carpenter, C. J. Cerjan, T. J. Clancy, T. Doeppner, M. J. Eckart, M. J. Edwards, S. Friedrich, S. H. Glenzer, S. W. Haan, E. P. Hartouni, R. Hatarik, S. P. Hatchett, O. S. Jones, G. Kyrala, S. Le Pape, R. A. Lerche, O. L. Landen, T. Ma, A. J. MacKinnon, M. A. McKernan, M. J. Moran, E. Moses, D. H. Munro, J. McNaney, H. S. Park, J. Ralph, B. Remington, J. R. Rygg, S. M. Sepke, V. Smalyuk, B. Spears, P. T. Springer, C. B. Yeamans, M. Farrell, D. Jasion, J. D. Kilkenny, A. Nikroo, R. Paguio, J. P. Knauer, V. Yu Glebov, T. C. Sangster, R. Betti, C. Stoeckl, J. Magoon, M. J. Shoup III, G. P. Grim, J. Kline, G. L. Morgan, T. J. Murphy, R. J. Leeper, C. L. Ruiz, G. W. Cooper and A. J. Nelson, *Rev. Sci. Instrum.* **83**, 10D308 (2012).

²⁹J. L. Kline, K. Widmann, A. Warrick, R. E. Olson, C. A. Thomas, A. S. Moore, L. J. Suter, O. Landen, D. Callahan, S. Azevedo, J. Liebman, S. H. Glenzer, A. Conder, S. N. Dixit, P. Torres III, V. Tran, E. L. Dewald, J. Kamperschroer, L. J. Atherton, R. Beeler Jr., L. Berzins, J. Celeste, C. Haynam, W. Hsing, D. Larson, B. J. MacGowan, D. Hinkel, D. Kalantar, R. Kauffman, J. Kilkenny, N. Meezan, M. D. Rosen, M. Schneider, E. A. Williams, S. Vernon, R. J. Wallace, B. Van Wonterghem and B. K. Young, *Rev. Sci. Instrum.* **81**, 10E321 (2010).

³⁰A G MacPhee, D H Edgell, E J Bond, D K Bradley, C G Brown, S R Burns, J R Celeste, C J Cerjan, M J Eckart, V Y Glebov, S H Glenzer, D S Hey, O S Jones, J D Kilkenny, J R Kimbrough, O L Landen, A J Mackinnon, N B Meezan, J M Parker and R M Sweeney, *J. Instrum.* **6**, P02009 (2011).

³¹M. A. Barrios, A. MacPhee, S. P. Regan, J. Kimbrough, S. R. Nagel, L. R. Benedetti, S. F. Khan, D. Bradley, P. Bell, D. Edgell and G. W. Collins, *Rev. Sci. Instrum.* **83**, 10E105 (2012)

³²D. L. Bleuel, C. B. Yeamans, L. A. Bernstein, R. M. Bionta, J. A. Caggiano, D. T. Casey, G. W. Cooper, O. B. Drury, J. A. Frenje, C. A. Hagmann, R. Hatarik, J. P. Knauer, M. Gatuz Johnson, K. M. Knittel, R. J. Leeper, J. M. McNaney, M. Moran, C. L. Ruiz and D. H. G. Schneider, *Rev. Sci. Instrum.* **83**, 10D313 (2012).

³³C. B. Yeamans, D. L. Bleuel and L. A. Bernstein, *Rev. Sci. Instrum.* **83**, 10D315 (2012).

³⁴D. T. Casey, J. A. Frenje, M. Gatuz Johnson, F. H. Séguin, C. K. Li, R. D. Petrasso, V. Yu. Glebov, J. Katz, J. P. Knauer, D. D. Meyerhofer, T. C. Sangster, R. M. Bionta, D. L. Bleuel, T. Döppner, S. Glenzer, E. Hartouni, S. P. Hatchett, S. Le Pape, T. Ma, A. MacKinnon, M. A. McKernan, M. Moran, E. Moses, H.-S. Park, J. Ralph, B. A.

Remington, V. Smalyuk, C. B. Yeamans, J. Kline, G. Kyrala, G. A. Chandler, R. J. Leeper, C. L. Ruiz, G. W. Cooper, A. J. Nelson, K. Fletcher, J. Kilkenny, M. Farrell, D. Jasion and R. Paguio, *Rev. Sci. Instrum.* **83**, 10D912 (2012).

³⁵R. Hatarik, J. A. Caggiano, V. Glebov, J. McNaney, C. Stoeckl and D. H. G. Schneider, *Plas. Fus. Res.: Regular Articles* **9**, 0001000 (2014).

³⁶H. Brysk, *Plasma Phys.* **15**, 611 (1973).

³⁷S. F. Khan; P. M. Bell; D. K. Bradley; S. R. Burns; J. R. Celeste; L. S. Dauffy; M. J. Eckart; M. A. Gerhard; C. Hagmann; D. I. Headley; J. P. Holder; N. Izumi; M. C. Jones; J. W. Kellogg; H. Y. Khater; J. R. Kimbrough; A. G. Macphee; Y. P. Opachich; N. E. Palmer; R. B. Petre; J. L. Porter; R. T. Shelton; T. L. Thomas; J. B. Worden, in Target Diagnostics Physics and Engineering for Inertial Confinement Fusion, eds. P. Bell and. G. P. Grim, Proc. SPIE 8505, 850505 (2012).

³⁸D. B. Sayre, L. A. Bernstein, J. A. Church, H. W. Herrmann and W. Stoeffl, *Rev. Sci. Instrum.* **83**, 10D905 (2012).

³⁹R. M. Malone, H. W. Herrmann, W. Stoeffl, J. M. Mack and C. S. Young, *Rev. Sci. Instrum.* **79**, 10E532 (2008).

⁴⁰S. M. Glenn, L. R. Benedetti, D. K. Bradley, B. A. Hammel, N. Izumi, S. F. Khan, G. A. Kyrala, T. Ma, J. L. Milovich, A. E. Pak, V. A. Smalyuk, R. Tommasini and R. P. Town, *Rev. Sci. Instrum.* **83**, 10E519 (2012).

⁴¹F. E. Merrill, D. Bower, R. Buckles, D. D. Clark, C. R. Danly, O. B. Drury, J. M. Dzenitis, V. E. Fatherley, D. N. Fittinghoff, R. Gallegos, G. P. Grim, N. Guler, E. N. Loomis, S. Lutz, R. M. Malone, D. D. Martinson, D. Mares, D. J. Morley, G. L. Morgan,

J. A. Oertel, I. L. Tregillis, P. L. Volegov, P. B. Weiss, C. H. Wilde and D. C. Wilson,
Rev. Sci. Instrum. **83**, 10D317 (2012).

⁴²D.C. Wilson, W.C. Mead, L. Disdier, M. Houry, J.-L. Bourgade, T.J. Murphy, *Nucl. Instr. Meth. Phys. Res. Sec. A*, **488**, 400 (2002).

⁴³K. I. Read, *Physica* **D12**, 45 (1984).

⁴⁴D. L. Youngs *Physica* **D12**, 32 (1984).

⁴⁵D. L. Youngs, *Physica* **D37**, 270 (1989).

⁴⁶S. W. Haan, *Phys. Rev. A* **39**, 5812 (1989).

⁴⁷C. Bellei, P. A. Amendt, S. C. Wilks, M. G. Haines, D. T. Casey, C. K. Li, R. Petrasso and D. R. Welch *Phys. Plasmas* **20**, 012701 (2013)

⁴⁸B. A. Hammel, H. A. Scott, S. P. Regan, C. Cerjan, D. S. Clark, M. J. Edwards, R. Epstein, S. H. Glenzer, S. W. Haan, N. Izumi, J. A. Koch, G. A. Kyrala, O. L. Landen, S. H. Langer, K. Peterson, V. A. Smalyuk, L. J. Suter, and D. C. Wilson, *Phys. Plasmas* **18**, 056310 (2011).

⁴⁹M. M. Marinak, S. G. Glendinning, R. J. Wallace, B. A. Remington, K. S. Budil, S. W. Haan, R. E. Tipton, and J. D. Kilkenny, *Phys. Rev. Lett.* **80**, 4426 (1998).

⁵⁰V. A. Smalyuk, M. Barrios, J. A. Caggiano, D. T. Casey, C. J. Cerjan, D. S. Clark, M. J. Edwards, J. A. Frenje, M. Gatu-Johnson, V. Y. Glebov, G. Grim, S. W. Haan, B. A. Hammel, A. Hamza, D. E. Hoover, W. W. Hsing, O. Hurricane, J. D. Kilkenny, J. L. Kline, J. P. Knauer, J. Kroll, O. L. Landen, J. D. Lindl, T. Ma, J. M. McNaney, M. Mintz, A. Moore, A. Nikroo, T. Parham, J. L. Peterson, R. Petrasso, L. Pickworth, J. E. Pino, K. Raman, S. P. Regan, B. A. Remington, H. F. Robey, D. P. Rowley, D. B. Sayre, R. E.

Tipton, S. V. Weber, K. Widmann, D. C. Wilson and C. B. Yeamans, *Phys. Plasmas* in press (2014).

Table I. DT capsule performance

metric	N120923	N120923 simulation	N130503	N130503 simulation	N130505	N130505 simulations	N130507	N130507 simulation
DT Y	6.7e14	1.08e15	5.1e14	5.48e14	8.0e14	1.12e15	7.3e14	1.45e15
DT Ti (keV)	3.3	3.06	4.62	4.83	2.72	2.99	2.81	3.14
DD Y	7.53e12	1.28e13	1.54e12	1.84e12	3e12	4.54e12	2.82e12	5.45e12
DD Ti (keV)	3.12	2.87	4.19	4.34	2.45	2.81	2.36	2.94
dsr (%)	1.1	1.0	0.24	0.10	1.16	1.00	1.06	1.11
γ BT (ns)	22.42	22.51	4.64	4.77	22.68	22.77	23.37	23.37
x-ray BT (ns)	22.47	22.52	4.90	4.88	22.83	22.79	23.46	23.39
γ BW (ps)	245	219		365	269	243	295	219
x-ray BW (ps)	243	243	373	208	380	302	313	239
x-ray P0 (μm)	44.3	51.3	181	182		57.4	40.1	50.5
x-ray P2/P0 (%)	-0.4	27	-2	1.1		53	-27.9	-14.7
n image P0 (μm)	46	48.2	100	106	50.3	51.3	39	46.3
n image P2/P0 (%)	-19	20	2		27	37	-28	-7.4

DT yield – yield of escaping neutrons in 13-15 MeV energy range, DT Ti – ion temperature inferred from width of 14 MeV neutron peak, DD Y – yield of escaping neutrons in 2.2-2.7 MeV energy range, DD Ti – ion temperature inferred from width of DD peak, dsr – down-scatter ratio, 10-12 MeV / 13-15 MeV neutrons; BT – bang time; BW – burn full width at half maximum; P0,P2 – Legendre modes of image contour at 17% of peak; neutron image metrics are for primary 14 MeV neutron image. Not all data exists for some shots.

Table II. D³He capsule performance

metric	N120909	simulation
DD Y	6.06e11	5.45e11
DD Ti (keV)	2.45	2.39
x-ray BT (ns)	22.59	22.48
x-ray BW (ps)	266	267
x-ray P0 (μ m)	51.0	47.2
x-ray P2/P0 (%)	4.8	-5.3

Items as in Table I.

FIGURE CAPTIONS

FIG. 1. Right-simulated density at bang time for nominal drive for the CD SymCap shot series, color scale as shown; left-normalized product of deuteron and tritium number densities at bang time for an ablator with a zero offset CD layer, color scale going from zero to one.

FIG. 2. (a) Simulated DT neutron yield vs. recess of the CD layer with (i) $f_b=0$, (ii) $f_b=0.04$, (iii) $f_b=0.08$, (iv) $f_b=0.16$. Shot data points are solid circles; two overlapping background shots with no CD layer plotted on left, simulation using $f_b=0.04$ as the open circle. In most cases, error bars are smaller than the symbols; (b) TT neutron yield vs. recess of the CD layer, symbols as in (a); (c) Ion temperature from 14 MeV DT peak vs recess of the CD layer, symbols as in (a).

FIG. 3. (a) Simulated primary neutron image of shot N120923; red line is 17% isocontour, scale is in cm. (b) Simulated x-ray image of shot N120923 at peak brightness through 2.5 mm kapton filter. (c) Experimental primary neutron image of N130923; scale is in μm . (d) Experimental x-ray image of N120923 at peak brightness through 2.5 mm kapton filter.

FIG. 4. Simulated DT an TT neutron yields vs. multiplier applied to nominal surface roughness for CD SymCap with zero layer offset, using best fit $f_b=0.04$. The dashed and dotted lines are the measure DT and TT yields, respectively.

FIG. 5. Simulated DT yield for shot N130507 as degradations are added progressively from 1-D clean, 2-d with surface roughness only, adding drive asymmetry, adding the tent mock-up, adding the mix model with $f_b=0.04$, and 2-d with all seeds and a different drive model developed by Dan Clark⁸. At the bottom is the measured DT yield.

FIG. 6. Simulated DT yield for shot N130507 vs. multiplier applied to nominal surface roughness. These results use a slightly different drive model than Fig. 5 and Table I. The observed yield is indicated with the dashed line.

FIG. 7. (a) Simulated x-ray image of D³He-filled SymCap, shot N120909, at peak x-ray emission, filtered with 2.5 mm kapton; (b) experimental x-ray image of N120909 at peak x-ray brightness. Contour levels are 17% of peak.

Figure 1

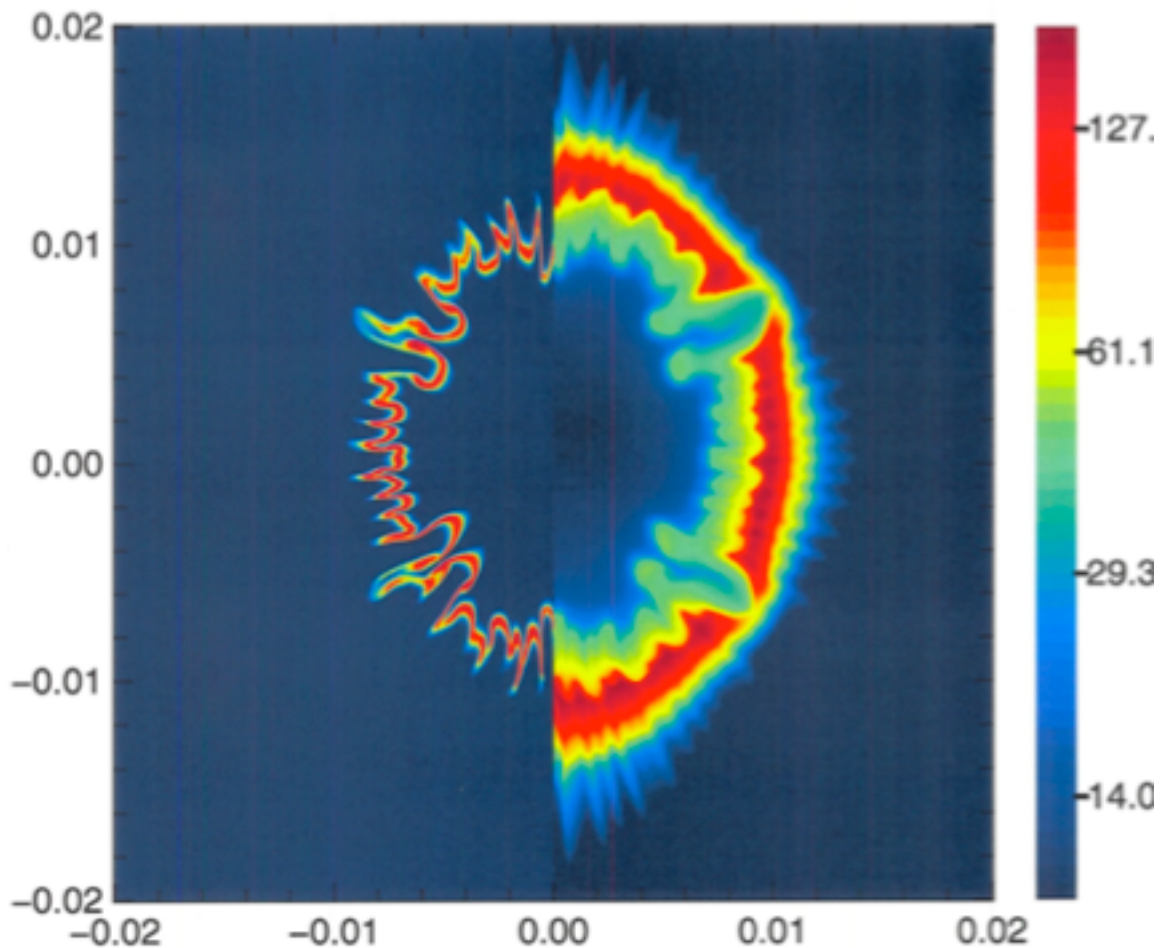
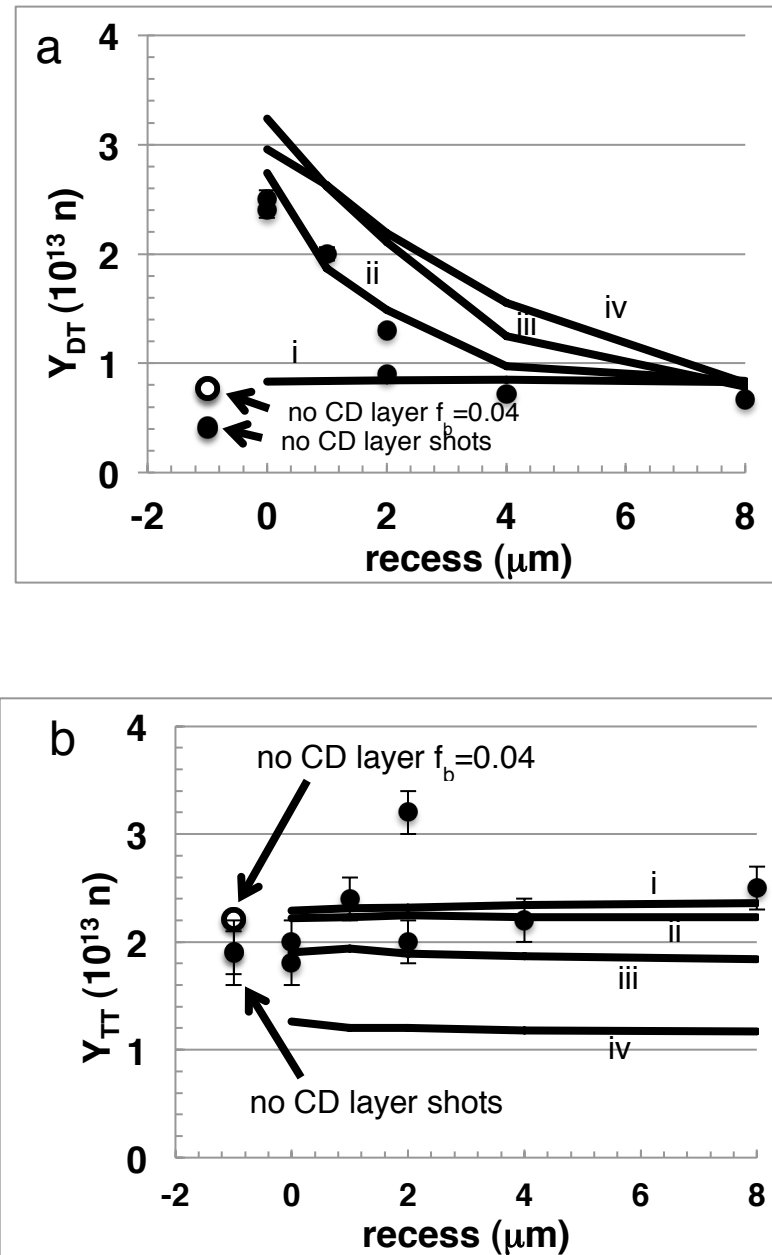


Figure 2



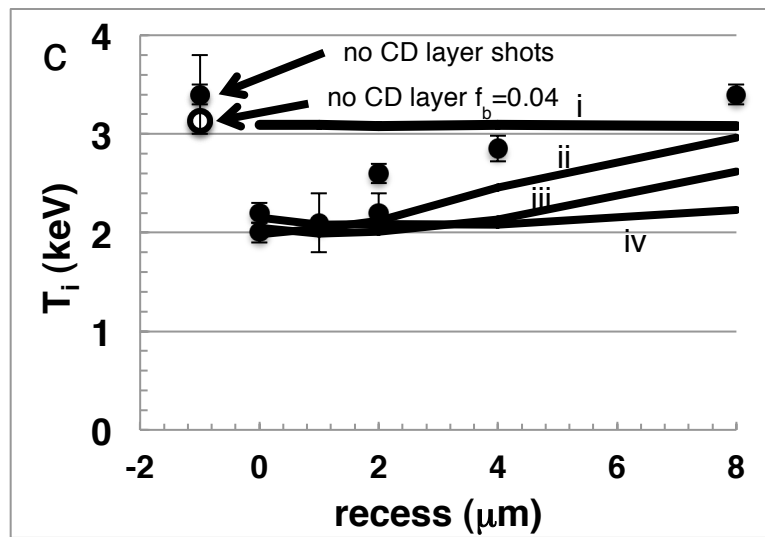


Figure 3

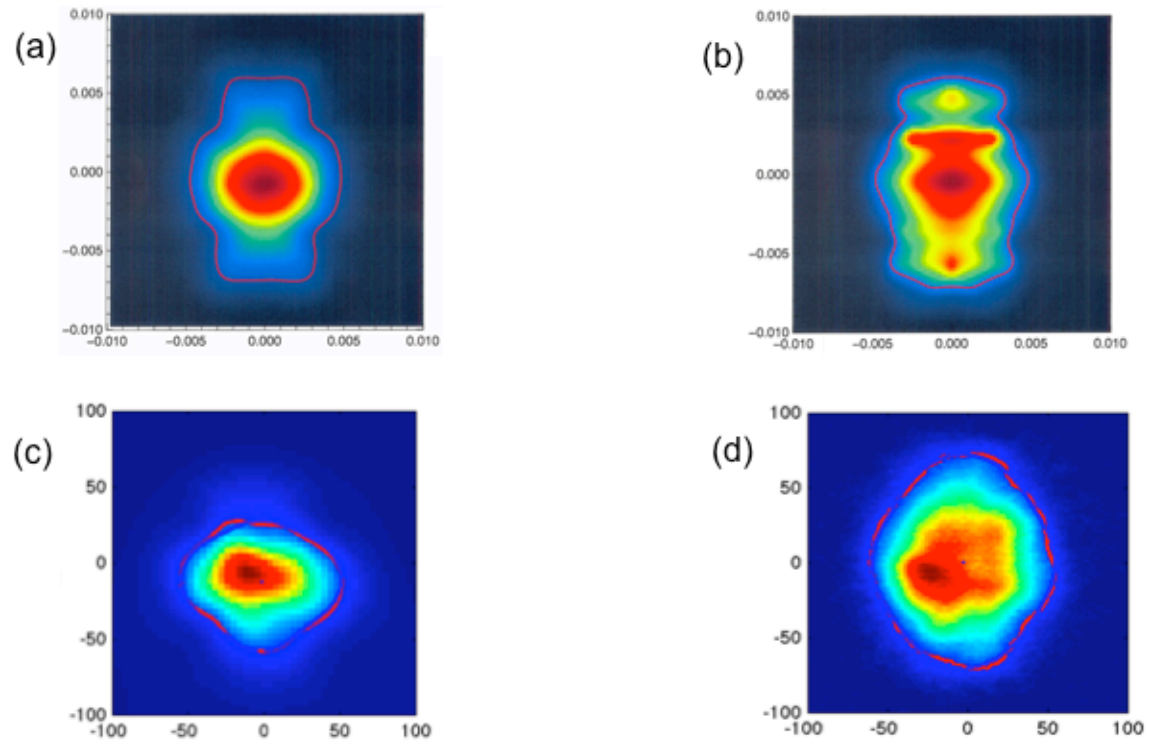


Figure 4

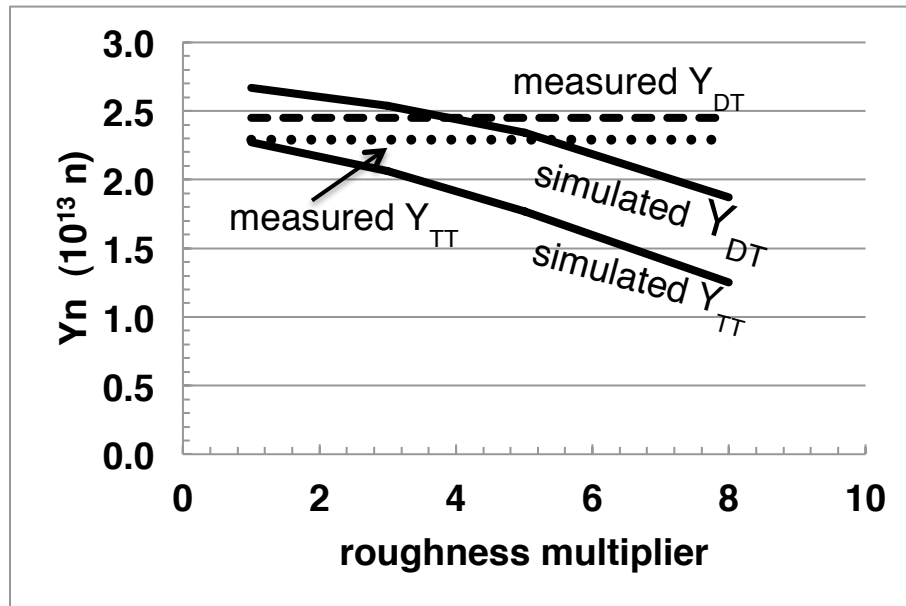


Figure 5

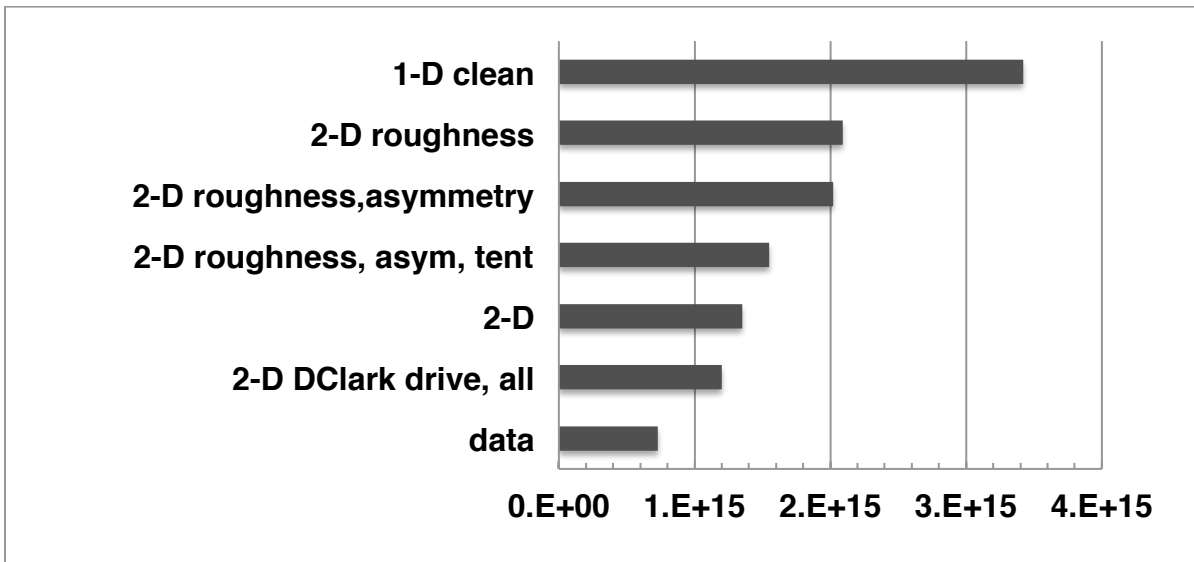


Figure 6

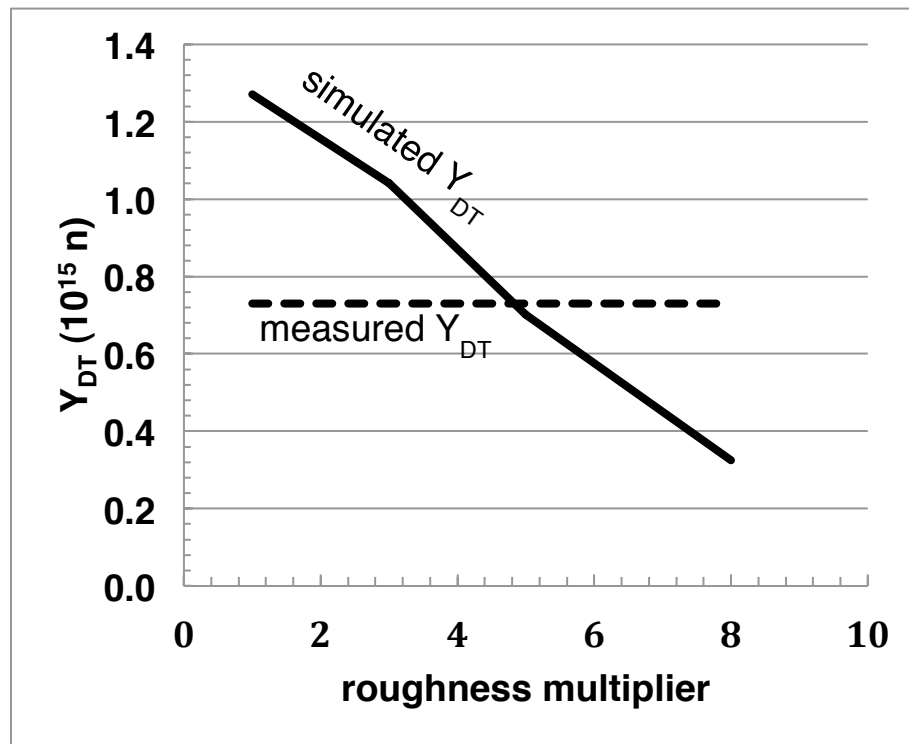


Figure 7

